# Supporting information

**Potassium Induced Stitching of Flexible Tripodal Ligand into Bi-metallic Two-dimensional Coordination Polymer for Photo-degradation of Organic Dyes**

Vimal K. Bhardwaj*

*Department of Chemistry, Indian Institute of Technology Ropar, Rupnagar, Punjab, 140001, India.*

*E-mail: vimalb@iitrpr.ac.in

**General.** All solvents were dried by standard methods. Unless otherwise specified, chemicals were purchased from commercial suppliers and used without further purification. The elemental analyses were performed on Perkin–Elmer 2400 CHN analyzer. I. R. spectra were recorded on a Bruker Tensor 27 spectrometer for the compounds in the solid state as KBr discs or as neat samples. The absorption spectra were recorded on a Lab-India and Shimadzu UV-1800, UV-vis Spectrophotometer. The PAN alytical X'PERT PRO diffractometer was used for X-ray diffraction (XRD) with a scan speed of $10^{o}$ $min^{-1}$ for $2\theta$ over a range from 10 to 80 (45 kV, 40 mA using Ni-fltered Cu $K_{\alpha}$ radiations). TGA measurements were made on a SII EXSTAR TGA thermo analyser instrument.

.

**X-ray structure determination.** The X-ray diffraction data were collected on a Bruker X8 APEX II KAPPA CCD diffractometer at 100 K using graphite monochromatized Mo-$K_{\alpha}$ radiation ($\lambda$ = 0.71073 Å). The crystals were positioned at 40 mm from the CCD and the diffraction spots were measured using a counting time of 10 s. Data reduction and multi-scan absorption were carried out using the APEX II program suite (Bruker, 2007). The structures were solved by direct methods with the SIR97 program[1] and refined using full-matrix least squares with SHELXL-97.[2] Anisotropic thermal parameters were used for all non-H atoms. The hydrogen atoms of C–H groups were with isotropic parameters equivalent to 1.2 times those of the atom to which they were attached. All other calculations were performed using the programs WinGX[3] and PARST.[4] The molecular diagrams were drawn with DIAMOND and OLEX2.[5] Two $CH_3CN$ molecules were located in the crystal structure however, only one of these molecules was present in short contact with the one of methylene hydrogen of the functionalized aminoethyl group of ligand. Other $CH_3CN$ displayed the disorder due to high thermal motions that could not be modeled. The contribution of this molecule was therefore removed by using mask in OLEX2 refinement program. [5]

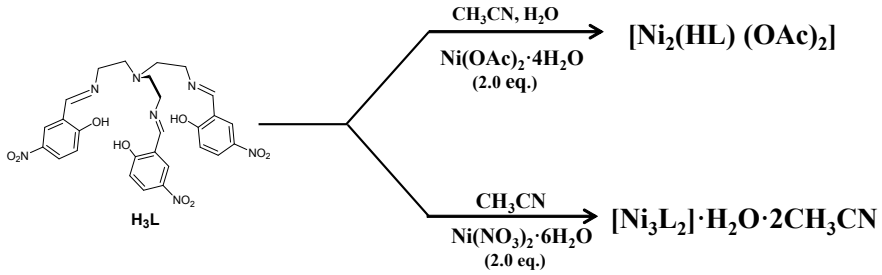


**Scheme S1**. Summarizing scheme showing synthetic routes of previously reported complexes $[Ni_2(HL)(OAc)_2]$ and $[Ni_3L^1{}_2]\cdot H_2O\cdot 2CH_3CN$

**Synthesis of {[K(NiL)]·*x*$CH_3CN$}$_n$ (1)**: The ligand $H_3L$ was prepared by literature procedure.[6] To a warm solution of **$H_3L^1$** (593 mg, 1.0 mmol) in acetonitrile, a solution of $Ni(OAc)_2\cdot 4H_2O$ (249 mg, 1.0 mmol) in water was added in the presence of KOH solution (84 mg, 1.5 mmol). The reaction mixture was refluxed for 2 h. Reddish brown solution was obtained which was filtered and suitable quality crystals were grown directly from the above solution by slow evaporation. Yield: 43 %. Anal. Calc. (%) for $C_{27}H_{24}N_7O_9NiK\cdot 2CH_3CN$: C, 48.33; H, 3.92; N, 16.36. Found: C, 48.38; H, 3.97; N, 16.41. IR (KBr, $cm^{-1}$): ν = 3255 (m), 2924 (w), 2924 (w), 2854 (m), 1657 (s), 1590 (s), 1543 (m), 1477 (m), 1439 (m), 1270 (s), 1161 (w), 1091 (m), 1093 (m), 911 (m), 836 (w), 755 (m), 719 (w), 697 (w), 605 (w).

Crystal data: $C_{29}H_{27}KN_8NiO_9$, $M_r$ = 729.40, triclinic, Space group *P*-1, $a$ = 10.6994(4), $b$ = 12.5806(5), $c$ = 14.3433(5) Å, $\alpha$ = 105.1090(10) °, $\beta$ = 93.3900(10) °, $\gamma$ = 93.6440(10) °, $V$ = 1854.42(12) $Å^3$, $Z$ = 2, $\rho_{calc}$ = 1.306 $g/cm^3$, $\mu$ = 0.692 $mm^{-1}$, $F(000)$ = 752.0, 8571 unique reflections ($R_{int}$ = 0.0222) out of 74033, GOF = 1.119, $R_1$/ $wR_2$ 0.0359/0.1159 (I>=2σ (I)), $R_1$/ $wR_2$ 0.0409/0.1193 (all data) with 8571 parameters and 434 restraints.

**Photo-catalytic experiments:**

Photo-catalytic activities of the samples for the decomposition of organic dyes were carried at ambient temperature (25° C). Typically, 20 mg of sample **1** was dispersed into 25 ml of (20

mg/L) methyl orange (MO) aqueous solution on a water bath, followed by the addition of few drops of 30 % hydrogen peroxide solution. A xenon arc lamp was used as the light resource. The suspensions were magnetically stirred for 30 min. At regular time intervals, 2ml solution of irradiated sampled was filtered and diluted to 3 times volume. The UV-Vis absorption spectra of prepared samples were recorded. The photo-catalytic activities of the sample **1** for the decomposition of MB were also evaluated by similar procedures. The rate of degradation was calculated by the slope of plot between $(C_0\text{-}C)/C_0$ and time, where $C_0$: original concentration of methyl orange and C: the concentration of methyl orange after degradation.

The photo-catalytic mechanism of **1** is shown below (Scheme S1). When the complex **1** was exposed to visible light irradiation, electrons (e-) in the valence band (VB) of **1** get excited to its conduction band (CB), leaving behind the holes ($h^+$) in VB. The electrons (e-) possess reducing character while the holes ($h^{+}$) have oxidation character. The electrons (e-) combine with $O_2$ adsorbed on the surfaces of **1** to generate the Oxygen radicals ($\cdot O_2^-$) that might transform to the hydroxyl radicals (·OH). Hydroxyl ($OH^-$) species adsorbed on the surfaces of **1** interact with the hole ($h^+$) to generate hydroxyl radicals (·OH). The generated hydroxyl radicals (·OH) could effectively decompose the organic dyes. It is observed that **1** initially shows the slow degradation of organic dyes that later becomes faster due to increase in the generation speed of hydroxyl radicals.

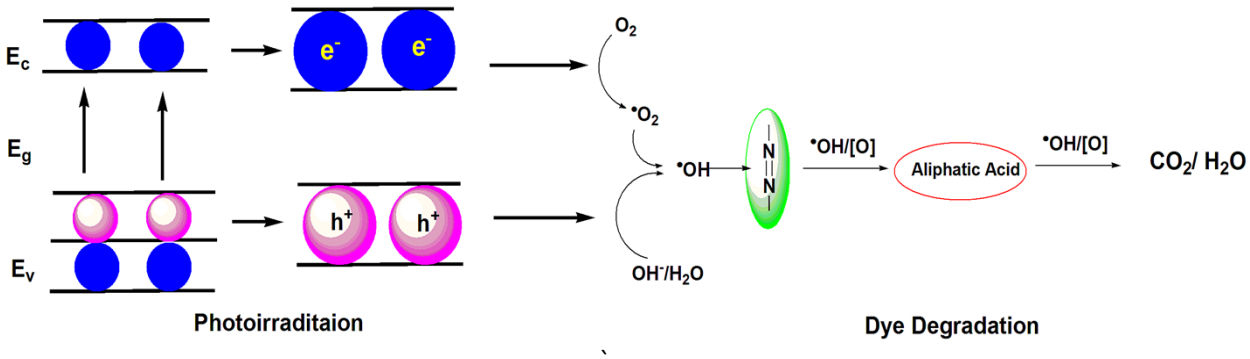


**Scheme S2**. Schematic diagram showing photo-catalytic mechanism of **1**.

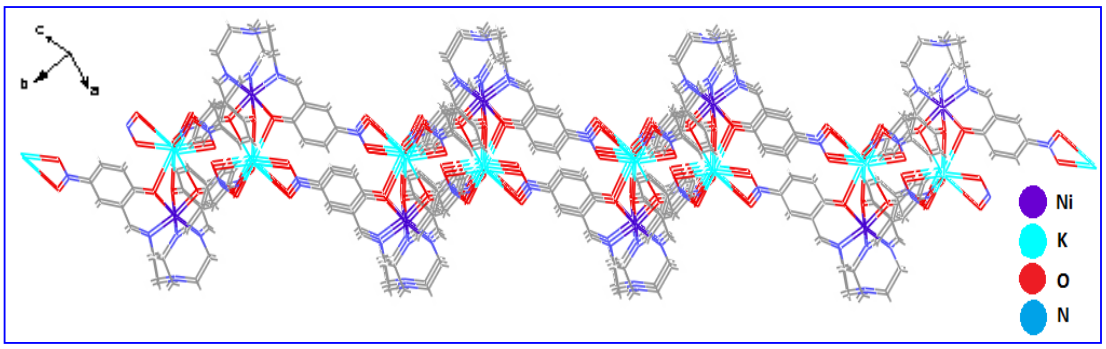


**Figure S1**. Stacking layer representation of complex $\{[K(NiL)]\bullet xCH_3CN\}_n$ (**1**), the solvent molecules are omitted.

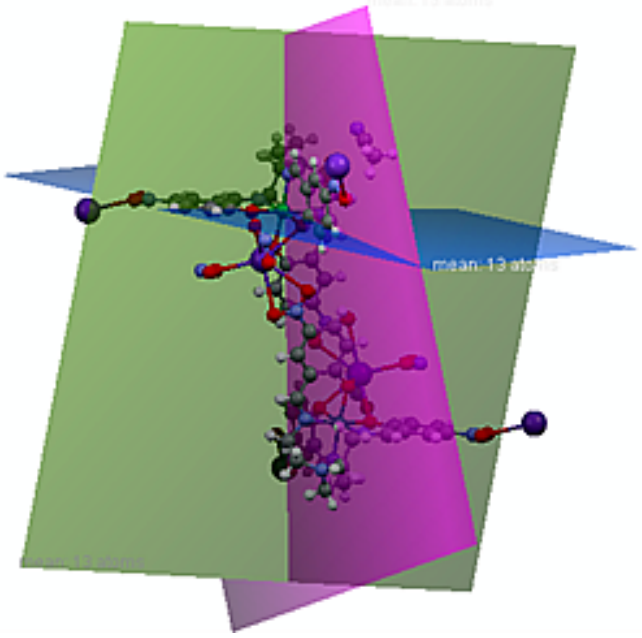

**Figure S2**. Showing the co-planarity of Ni(II) with all the three nitrophenolate rings in complex **1**.

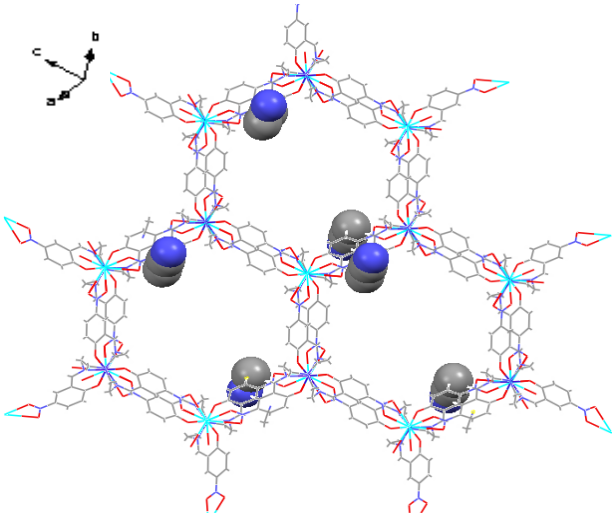

**Figure S3.** Packing diagram of (**1**) showing solvent molecules in the voids of supramolecular assembly. Host framework is presented in a wireframe style while the solvates are presented with a space-filling model. Hydrogen atoms are omitted.

**Thermal stability study**

The compound was stable enough to retain its crystalline nature at room temperature. The thermo gravimetric analysis (TGA) was performed for the crystalline sample of the complex in the range of 30–1000 °C under a flow of nitrogen (figure S4). The result shows that the compound was stable up to 300 °C, however a gradual weight loss of 9.87 % in the temperature range of 50-280 °C, was observed corresponding to the loss of non-coordinated acetonitrile molecules (calcd. 10.64 %). This indicates the weak interactions between complex and solvent. Above 300 °C decomposition of organic ligand occurs gradually up to 850 °C followed by appearance of 19.04 % of residue. The residue obtained is indicative of NiO and $K_2O$ mixture (calcd. 20.8 %) formation.

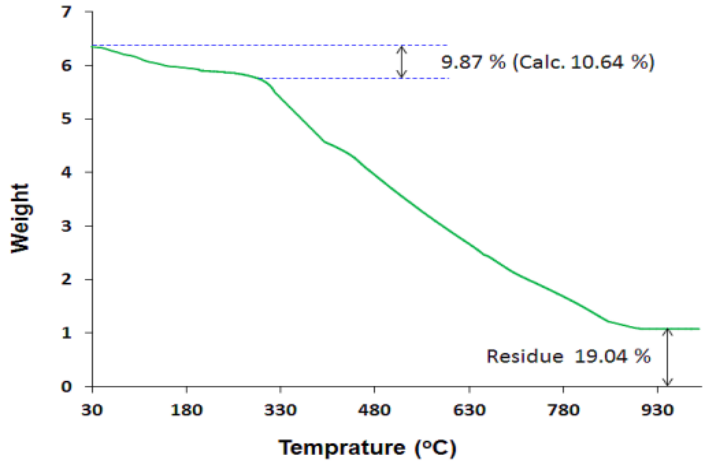


**Figure S4**. TGA for **1** in temperature range of 30 to 1000 °C at the heating rate of 10 °C / min under the $N_2$ atmosphere.

**Water stability study**

The bulk sample was treated with deionized water for 24 h and was finally washed with acetone. The powder X-ray diffraction pattern of pure sample 1 and water treated sample of 1 are nearly identical with no new peak (figure S5); however some loss in the intensity of 2θ values was observed. Therefore this is evident that the crystal lattice remains intact after being treated with water.

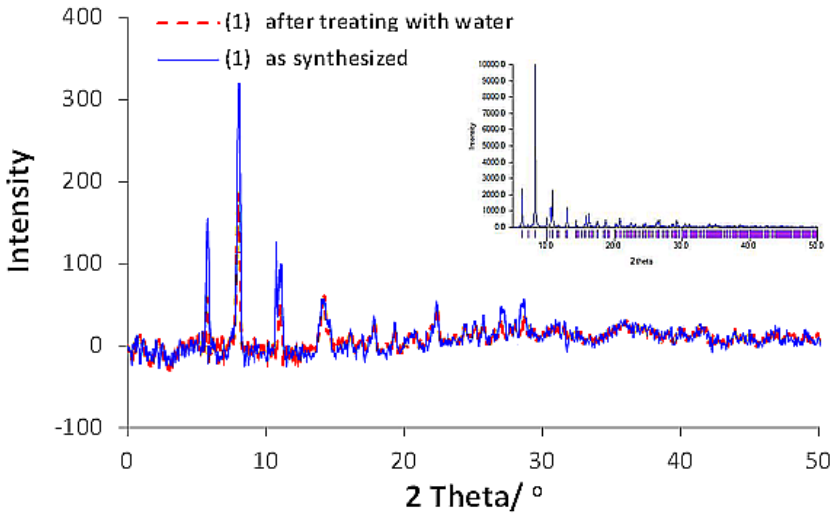


**Figure S5**. Powder X-ray diffraction pattern of $\{[K(NiL)]\bullet xCH_3CN\}_n$ (**1**) as synthesized and after treating water for 24 h. Inset: simulated pattern from single crystal data of **1.**

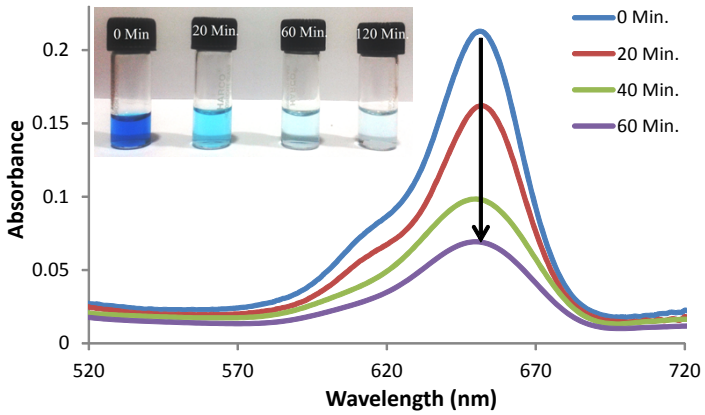


**Figure S6**. Changes of the UV-Vis spectra of MB in the presence of **1** after light illumination from 0 to 60 min. (Inset) Photograph showing the photo-catalytic degradation of MB under UV-visible light for different time intervals.

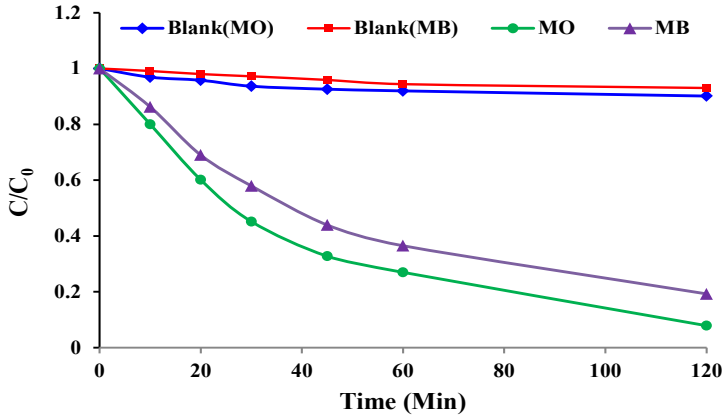


**Figure S7**. The comparative photo-catalytic profiles (plot of concentration of dye versus reaction time) for MO and MB in the absence (Blank) and presence of metal complex **1**.

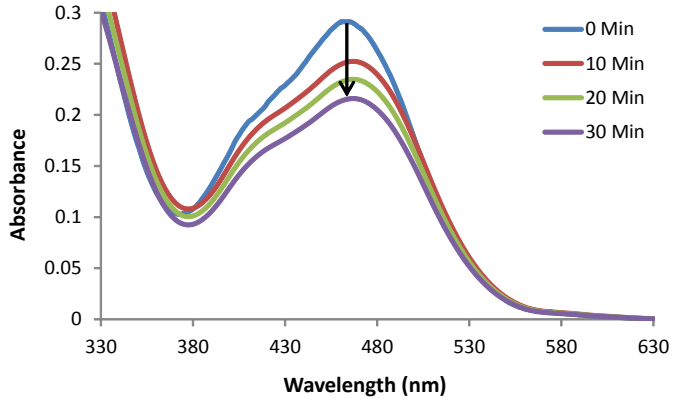


**Figure S8**. Changes of the UV-Vis spectra of MO in the presence of previously reported $H_3L$ type complex $[Ni_2(HL_1)(OAc)_2]$ after light illumination from 0 to 30 min.

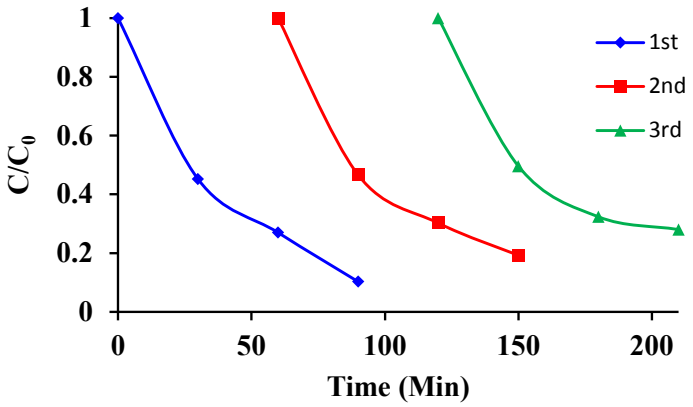


**Figure S9**. Recycling test of complex **1** for MO photo-degradation under light irradiation.

**Table S1.** Selected bond lengths and angles (Å,°) for $\{[K(NiL)]\cdot x CH_3CN\}_n$ (**1**)

| | | | | | |
|---|---|---|---|---|---|
| Bond lengths (Å) | | | | | |
| N(2)-Ni(1) | 2.1036(13) | N(5)-K(1) | 3.2777(15) | O(5)-K(1) | 2.9259(14) |
| N(3)-Ni(1) | 2.1071(13) | N(6)-K(1) | 3.3360(17) | O(6)-K(1) | 2.9513(17) |
| N(4)-Ni(1) | 2.0920(13) | N(7)-K(1) | 3.3073(17) | O(7)-K(1) | 2.9732(18) |
| O(1)-Ni(1) | 2.0325(11) | O(2)-K(1) | 2.7944(12) | O(8)-K(1) | 2.9738(16) |
| O(2)-Ni(1) | 2.0555(11) | O(3)-K(1) | 2.7946(12) | O(9)-K(1) | 2.9038(17) |
| O(3)-Ni(1) | 2.0555(11) | O(4)-K(1) | 2.8741(15) | | |
| Bond angles(°) | | | | | |
| N(5)-K(1)-N(6) | 102.66(4) | O(2)-K(1)-O(7) | 83.84(5) | N(2)-Ni(1)-K(1) | 118.29(4) |
| N(5)-K(1)-N(7) | 110.17(5) | O(2)-K(1)-O(8) | 116.61(5) | N(4)-Ni(1)-N(2) | 98.59(5) |
| N(7)-K(1)-N(6) | 114.83(5) | O(2)-K(1)-O(9) | 74.67(5) | N(4)-Ni(1)-N(3) | 100.01(5) |
| O(1)-K(1)-N(5) | 84.84(4) | O(3)-K(1)-N(5) | 96.62(4) | N(4)-Ni(1)-K(1) | 119.90(4) |
| O(1)-K(1)-N(6) | 93.20(5) | O(3)-K(1)-N(6) | 145.91(4) | N(3)-Ni(1)-K(1) | 117.21(4) |
| O(1)-K(1)-N(7) | 142.94(4) | O(3)-K(1)-N(7) | 83.56(4) | O(1)-Ni(1)-N(2) | 88.62(5) |
| O(1)-K(1)-O(2) | 60.41(3) | O(3)-K(1)-O(4) | 75.70(4) | O(1)-Ni(1)-N(4) | 170.87(5) |
| O(1)-K(1)-O(3) | 60.62(3) | O(3)-K(1)-O(5) | 118.58(4) | O(1)-Ni(1)-N(3) | 84.29(5) |
| O(1)-K(1)-O(4) | 80.29(4) | O(3)-K(1)-O(6) | 159.14(5) | O(1)-Ni(1)-O(3) | 86.52(4) |
| O(1)-K(1)-O(5) | 95.34(4) | O(3)-K(1)-O(7) | 130.53(5) | O(1)-Ni(1)-O(2) | 85.97(4) |
| O(1)-K(1)-O(6) | 114.45(5) | O(3)-K(1)-O(8) | 93.89(4) | O(1)-Ni(1)-K(1) | 51.18(3) |
| O(1)-K(1)-O(7) | 72.66(4) | O(3)-K(1)-O(9) | 80.14(5) | O(3)-Ni(1)-N(2) | 85.89(5) |
| O(1)-K(1)-O(8) | 153.05(4) | O(4)-K(1)-N(5) | 21.89(4) | O(3)-Ni(1)-N(3) | 88.40(5) |
| O(1)-K(1)-O(9) | 130.43(5) | O(4)-K(1)-N(6) | 124.08(4) | O(3)-Ni(1)-N(4) | 169.55(5) |
| O(2)-K(1)-N(5) | 144.18(4) | O(4)-K(1)-N(7) | 101.00(5) | O(3)-Ni(1)-O(2) | 86.22(5) |
| O(2)-K(1)-N(6) | 88.62(4) | O(4)-K(1)-O(6) | 124.68(5) | O(3)-Ni(1)-K(1) | 52.59(3) |
| O(2)-K(1)-N(7) | 94.91(5) | O(4)-K(1)-O(7) | 112.93(5) | O(3)-Ni(1)-N(2) | 170.69(5) |
| O(2)-K(1)-O(4) | 60.23(3) | O(4)-K(1)-O(8) | 85.14(6) | O(2)-Ni(1)-N(3) | 86.12(5) |
| O(2)-K(1)-O(5) | 153.87(4) | O(4)-K(1)-O(9) | 120.03(5) | O(2)-Ni(1)-N(4) | 88.17(5) |
| O(2)-K(1)-O(6) | 99.24(5) | N(2)-Ni(1)-N(3) | 98.84(5) | O(2)-Ni(1)-K(1) | 52.59(3) |

1. Altomare, M. C. Burla, M. Camalli, G. L. Cascarano, C. Giacovazzo, A. Guagliardi, A. G. G. Moliterni, G. Polidori, R. Spagna, *J. Appl. Crystallogr.,* 1999, **32**, 115.
2. G. M. Sheldrick, *Acta Crystallogr., A* 2008*,* **64**, 112.
3. L. J. Farrugia, *J. Appl. Crystallogr.,* 1999, **32**, 837.
4. M. Nardelli, *J. Appl. Crystallogr.,* 1995, **28**, 659.
5. (a)W. T. Pennington, *J. Appl. Cryst.,* 1999, **32**, 1028; (b) O.V. Dolomanov, L. J. Bourhis, R. J. Gildea, J. A. K. Howard, H. Puschmann, *J. Appl. Cryst.,* 2009, **42**, 339.
6. W. Schilf, B. Kamieński, B. Kołodziej, E. Grech, E. *J. Mol. Structure,* 2004, **708**, 33–38.